

Dynamical characterization in different slow quenching processes

Panpan Fang¹, Yi-Xiang Wang^{1,2,*} and Fuxiang Li^{1†}

¹*School of Physics and Electronics, Hunan University, Changsha 410082, China and*

²*School of Science, Jiangnan University, Wuxi 214122, China*

(Dated: September 15, 2022)

Dynamical characterization plays an important role in characterizing the bulk topology of equilibrium topological phases. In this paper, we investigate all possible quenching processes of the two-dimensional Chern insulator under slow nonadiabatic quench dynamics. Different types of zero polarizations including initial spin inversion surface, final spin inversion surface, and final band inversion surface, are founded in the time-averaged spin polarization. Each quenching process shows its unique features to these zero polarizations, on which the winding of the dynamical field exactly reflects the topological invariants of the system. No matter how the quenching process is, the time-averaged spin polarization only records the topological invariants of the initial phase and final phase. Importantly, compared with the sudden quench, the initial phase and final phase can be distinguished by the difference between initial spin inversion surface, final spin inversion surface, and final band inversion surface. In addition, we show the above findings are robust to an arbitrary initial state. All the dynamical characterization schemes in the different quenching processes are entirely based on the experimentally measurable quantity time-averaged spin polarization, and thus one can expect our findings may provide reference for future experiments.

I. INTRODUCTION

Topological quantum phases have been extensively studied in last two decades [1–8]. Under the equilibrium theory, the topological quantum phases can be classified and characterized by its topological invariants defined with Bloch functions. The tightness of the topological invariants and robust boundary modes immune to moderate disorder or defects, is called the famous bulk-boundary correspondence. According to the bulk-boundary correspondence, one can identify the topological phases by resolving the boundary modes with angle-resolved photoelectron spectroscopy and transport measurements experimentally [9–12]. In addition to the equilibrium theory, the notion of characterizing topological phases can also be extended to the nonequilibrium theory.

Nonequilibrium theory plays an important role in characterizing topological properties of equilibrium topological phases such as (non-) Hermitian quantum systems, (non-) correlated systems, higher-order (lower-order) topological insulators, etc [13–23]. Recently, a dynamical bulk-surface correspondence, which states a generic dD topological phase can be characterized by the $(d-1)$ D invariant defined on the so-called band inversion surface (BIS), is established by Liu and his co-workers in Hermitian systems [24, 25]. Due to the platforms of well-designed optical lattice in ultracold atomic systems, the measurement of the time-averaged spin polarization (TASP) by spin-resolved time-of-flight absorption imaging becomes possible. Thus, this dynamical bulk-surface correspondence is further verified experimentally [26–30]. In momentum-space, after suddenly quenching the system from a deep trivial phase to a topological phase, the bulk topology of a dD equilibrium phase of the postquench Hamiltonian can be easily determined with high-precision by the winding of dynamical field on BIS in the TASP.

Compared with the sudden quench, a general dynamical characterization scheme based on the slow quench protocol is provided in our previous works [31, 32]. It has been found that, nonadiabatic slow quench dynamics can indeed provide an alternative position named spin inversion surface (SIS) in characterizing the topological phases. However, the previous studies only consider the dynamical characterization in one type of quenching process, which makes the system slowly quench from a deep trivial phase to a topological phase. One may wonder whether it is critical for dynamical characterization to quench from a topologically trivial phase. What knowledge could we obtain by reversing the quenching processes (i.e. from “topological set of parameters” to “non-topological ones”) or by quenching between regimes with different topological invariants? Moreover, the initial state of the previous studies was only set as the ground state of the initial phase, and the influence of the initial state has not been considered yet. Under an arbitrary initial state with the system being slowly quenched in all the possible quenching processes, one would obtain a more general rule of the dynamical characterization and provide more reference for future experiments.

In this paper, in the framework of slow nonadiabatic quench, we uncover a general rule of the dynamical characterization in different quenching processes of the two-dimensional Chern insulator. By analyzing the precession behavior of the spin polarization under the slow quench dynamics, we find that there exist three typical zero polarizations in TASP, namely, initial spin inversion surface (ISIS), final spin inversion surface (FSIS), and final band inversion surface (FBIS). Then after obtaining the TASP in different types of quenching processes, we show the winding of the dynamical field on these zero polarizations exactly reflects the topological invariants of the system. Each quenching process shows its unique features to these zero polarizations. Specifically, if only the paired zero polarizations (FBIS and FSIS) emerges in the TASP, the final phase of the system will be characterized. On the contrary, if only ISIS emerges in the TASP, the initial phase of the system will be characterized. In addition, if all the types of

* wangyixiang@jiangnan.edu.cn

† fuxiangli@hnu.edu.cn

zero polarizations exist in the TASP, both initial and final phases can be characterized. No matter how the quenching process is, the TASP only captures the topological invariants of the initial phase and final phase. Compared with the sudden quench, the initial phase and final phase can be distinguished by the difference between these zero polarizations. Finally, the robustness of the above results to an arbitrary initial state is also verified. All the dynamical characterization schemes are entirely based on the TASP, which can be observed directly in experiment. Therefore, one can expect our findings may provide reference for future experiments.

The rest of this paper is organized as follows. In Sec. II, we introduce the generic method of characterizing bulk topology under slow non-adiabatic quench dynamics. Then in Sec. III, we present the results of dynamical characterization in different quenching processes. Then we verify the robustness of the results to an arbitrary initial state in Sec. IV. Finally, we provide a brief discussion and summary to the main results of the paper in Sec. V and Sec. VI, respectively.

II. NONADIABATIC QUENCH DYNAMICS TO CHARACTERIZE THE TOPOLOGICAL PHASES

A. Nonadiabatic slow quench protocol

We first give a general introduction to the slow quench protocol that can be utilized in the non-adiabatic dynamical characterization of topological phases. In general, the Hamiltonian in momentum space is described in the following form

$$\mathcal{H}(\mathbf{k}, t) = \mathbf{h}(\mathbf{k}, t) \cdot \boldsymbol{\gamma} = \sum_{i=0}^d h_i(\mathbf{k}, t) \gamma_i. \quad (1)$$

The matrices $\boldsymbol{\gamma}$ satisfy the anticommutation relations $\{\gamma_i, \gamma_j\} = 2\delta_{ij}$ and are of dimensionality $n_d = 2^{d/2}$ (or $2^{(d+1)/2}$) when d is even (or odd). In 1D and 2D systems, $\boldsymbol{\gamma}$ are the Pauli matrices. In higher dimensional systems, $\boldsymbol{\gamma}$ take the Dirac form.

Here, we consider a specific protocol like $h_0(\mathbf{k}, t) = g/t + h_0(\mathbf{k})$ with g determines the quenching rate. The parameter g varies from 0 to ∞ , corresponding to a continuous crossover from the sudden quench limit ($g = 0$) to the adiabatic limit ($g \rightarrow \infty$). In such a protocol, the form of g/t enables us to quench the system from an initial Hamiltonian at $t = t_i$ to a final (postquench) Hamiltonian at $t = t_f$ by keeping other parameters unchanged. During the quenching process, the evolution of the state vector is fully determined by the Schrödinger equation $i\hbar \frac{d}{dt} |\psi(\mathbf{k}, t)\rangle = \mathcal{H} |\psi(\mathbf{k}, t)\rangle$ after preparing an initial state $|\psi(\mathbf{k}, t_i)\rangle$. Then the final TASP over a long time ($t_f - t_i$) at each \mathbf{k} point can be obtained as:

$$\overline{\langle \boldsymbol{\gamma}(\mathbf{k}) \rangle} = \frac{1}{t_f - t_i} \int_{t_i}^{t_f} \langle \psi(\mathbf{k}, t) | \boldsymbol{\gamma} | \psi(\mathbf{k}, t) \rangle dt. \quad (2)$$

B. The dynamical topological characterization under slow nonadiabatic quench dynamics

The dynamical topological characterization depends on the winding of the dynamical field on the zero polarizations appeared in the component of TASP $\overline{\langle \boldsymbol{\gamma}_0(\mathbf{k}) \rangle}$. Generally speaking, the formation of zero polarizations can be explained from the quench dynamics. The quench dynamics leads to a precession of the pseudospin $\langle \boldsymbol{\gamma}(\mathbf{k}, t) \rangle$ about the effective field $\mathbf{h}(\mathbf{k}, t)$, and one can observe an approximately stable dynamic precession behavior of pseudospin $\langle \boldsymbol{\gamma}(\mathbf{k}, t) \rangle$ after a certain time $\Delta t [g/(t_i + \Delta t) \ll h_0(k)]$. Thus, there may be two typical reasons for the formation of the zero polarizations in $\overline{\langle \boldsymbol{\gamma}_0(\mathbf{k}) \rangle}$: (i) the pseudospin $\langle \boldsymbol{\gamma}(\mathbf{k}, t) \rangle$ is perpendicular to the effective field $\mathbf{h}(\mathbf{k}, t)$, (ii) the pseudospin $\langle \boldsymbol{\gamma}(\mathbf{k}, t) \rangle$ is not perpendicular to the effective field $\mathbf{h}(\mathbf{k}, t)$, however, the component of pseudospin $\langle \boldsymbol{\gamma}_0(\mathbf{k}, t) \rangle$ oscillates between positive and negative value.

In addition, in order to obtain the TASP (then the zero polarizations in the TASP can be obtained), one can consider a famous Landau-Zener problem. Specifically, for a two-level system, if one prepare an initial state $|\psi(\mathbf{k}, t_i)\rangle$, the system will undergo a non-adiabatic transition during the evolution, and finally at time $t = t_f$, the system will not only stay on the final ground state $|-\rangle$ with probability $P_d(\mathbf{k})$, but also on the excited state $|+\rangle$ with probability $P_u(\mathbf{k})$. One can find the zero polarizations in all components of TASP on the momentum point with $P_u - P_d = 0$, i.e., the points where the excited state and the ground state have equal probabilities. Here, we define the position with $P_u - P_d = 0$ as SIS. Thus, the spin polarizations on the SIS also have same features as (i) described. We also define the position of the spin polarizations in (ii) as FBIS, on which only one component of TASP $\overline{\langle \boldsymbol{\gamma}_0(\mathbf{k}) \rangle}$ is zero. Surprisingly, the SIS can be subdivided into two types: one is FSIS discussed in previous paper, and its position is close to the FBIS; the other is ISIS, and its position is far away from the FBIS. Therefore, all the positions of these zero polarizations will be identified by the TASP itself, which can be directly measurable in experiment.

After identifying the zero polarizations in TASP, one can then obtain the dynamical field on the ISIS, FSIS and FBIS. On the ISIS and FSIS, all the components of TASP vanish, one needs to define a new field $\widetilde{g}_{so,i} = -\partial_{k_\perp} \overline{\langle \boldsymbol{\gamma}_{so,i}(\mathbf{k}) \rangle}$ to characterize the topology, while on the FBIS, one can characterize the topology by simply measuring the value of TASP $\overline{\langle \boldsymbol{\gamma}_{so,i}(\mathbf{k}) \rangle}$. Both the dynamical field $\overline{\langle \boldsymbol{\gamma}_{so,i}(\mathbf{k}) \rangle}$ and $\widetilde{g}_{so,i}$ can be shown to be proportional to the spin-orbit field $h_{so,i}$ (see Appendix A). Here, the spin-orbit field mean the remaining components of \mathbf{h} except $h_0(\mathbf{k}, t)$, and $\overline{\langle \boldsymbol{\gamma}_{so,i}(\mathbf{k}) \rangle}$ means one of the remaining components of TASP except $\overline{\langle \boldsymbol{\gamma}_0(\mathbf{k}) \rangle}$. Finally, one can easily capture the topological information of the system from the winding of \mathbf{h}_{so} on the ISIS and FSIS (FBIS), corresponding to the bulk topological invariants of the initial Hamiltonian $\mathcal{H}(t_i)$ and the final Hamiltonian $\mathcal{H}(t_f)$, respectively. For clarity, we summarize all the zero polarizations and their information in Table I. The information related to the BIS and SIS is always marked in purple and green in the following

description, respectively.

TABLE I. The comparison of ISIS, FSIS and FBIS.

Name	Bulk topology	Effective field	Position in TASP	Transition Probability
ISIS	Initial	$h(\mathbf{k}, t) \perp \langle \gamma(\mathbf{k}, t) \rangle$	Far away from BIS	$P_u - P_d = 0$
FSIS	Final	$h(\mathbf{k}, t) \perp \langle \gamma(\mathbf{k}, t) \rangle$	Close to BIS	$P_u - P_d = 0$
FBIS		$h(\mathbf{k}, t) \perp \langle \gamma(\mathbf{k}, t) \rangle$	$\langle \gamma_0(\mathbf{k}) \rangle = 0$	$P_u - P_d \neq 0$

III. DIFFERENT QUENCHING PROCESSES

Now we apply different quenching processes to the 2D Chern insulator, which is generically described by a two-band Hamiltonian spanned by three Pauli matrices: $\mathcal{H}(\mathbf{k}, t) = \mathbf{h}(\mathbf{k}, t) \cdot \boldsymbol{\sigma}$, with the vector field given by:

$$h_0(\mathbf{k}, t) \equiv h_z = \frac{g}{t} + m_z - t_0 \cos k_x - t_0 \cos k_y, \quad (3)$$

$$h_1 = h_x = t_{so} \sin k_x, \quad (4)$$

$$h_2 = h_y = t_{so} \sin k_y. \quad (5)$$

This Hamiltonian without time-dependent term g/t has been realized in recent experiment of quantum anomalous Hall effect [35]. Here, we slowly quench the z -component of vector field from $t = t_i$ to t_f (a large number compared with g), and study the emergent topological characterization after quenching. For $0 < g/t + m_z < 2t_0$, the Hamiltonian gives a topological phase with Chern number $\mathcal{C} = -1$. In addition, for $-2t_0 < g/t + m_z < 0$, the Hamiltonian describes a topologically nontrivial phase with Chern number $\mathcal{C} = +1$.

A. quench starts from a trivial phase to a topological phase

The exact solutions of the Landau-Zener problem are difficult to find and only a few special classes can be solved exactly. In the previous papers [31, 32], we have given an exact solutions in a special case. Briefly speaking, we slowly quench the system from a deep trivial phase (far from the phase boundary) to a topological phase with time t varies from $t_i \rightarrow 0$ to $t_f \rightarrow \infty$, and the initial state $|\psi(0)\rangle$ is always the ground state of the initial Hamiltonian $\mathcal{H}(t_i \rightarrow 0)$. Under these conditions, the TASP can be given by

$$\overline{\langle \sigma_i \rangle} = (P_u - P_d) \frac{h_i}{\varepsilon} = \frac{(e^{-2\pi g \frac{h_0}{\varepsilon}} - \cosh 2\pi g) h_i}{\sinh 2\pi g} \frac{1}{\varepsilon}. \quad (6)$$

with ε is the energy of final Hamiltonian $H(t_i \rightarrow \infty)$. Here, we still slowly quench the system from a trivial phase to a topological phase, however, the initial trivial phase is close to the phase boundary with $t_i \neq 0$.

As shown in Figs. 1(a), 1(b), and 1(c), we plot the three components of TASP after quenching the h_z axis from a trivial phase to a topological phase with topological invariant -1 . Similar to the quench starts from a deep trivial phase, the purple ring is identified as FBIS, on which only one component of

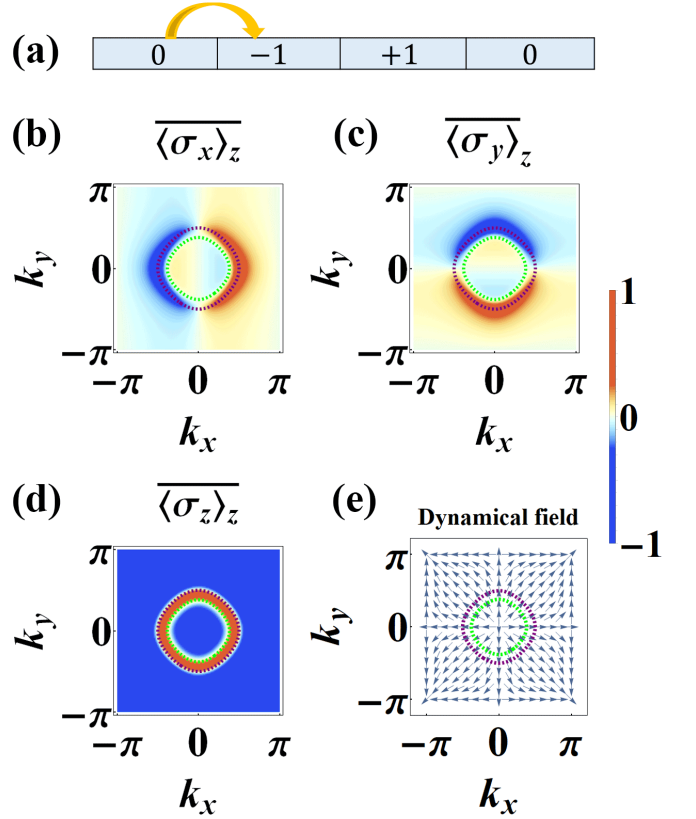


FIG. 1. (a) The specific quenching processes of slow quench. "0" represents the trivial phase, and other numbers represent the topological phase with different topological invariant. (b)-(d) The TASP after quenching h_z axis from a trivial phase to a topological phase with $\mathcal{C} = 1$. The system is quenched from $t_i = 1/2$ to $t_f = 5000$ with $5t_{so} = t_0 = g = m_z = 1$. The quench protocol is g/t and the initial state is the ground state of $\mathcal{H}(t_i)$. $\overline{\langle \sigma_z \rangle_z}$ represents the z component of TASP after quenching h_z axis, and so on. The green dashed line (inner ring) and purple dashed line (outer ring) represent the positions of FSIS and BIS, respectively. (e) The dynamical field of the system plotted by the normalized spin-orbit field \hat{h}_{so} .

TASP have vanishing polarizations. The green ring in $\overline{\langle \sigma_z \rangle}$ is identified as FSIS, on which all three components of TASP have vanishing polarizations. As the dynamical field plotted in Fig. 1(e), both the winding of the dynamical field on BIS and FSIS can characterize the bulk topology of final Hamiltonian.

In Figs. 2(a), 2(b), and 2(c), the three components of TASP are shown after quenching the h_z axis from a trivial phase to a topological phase with topological invariant $+1$. The purple lines and the green lines in $\overline{\langle \sigma_z \rangle}$ are also identified as FBIS and FSIS, respectively. Compared with the dynamical field shown in Fig. 1(e), the dynamical field plotted in Fig. 2(e) converges at a central point inside FBIS and FSIS rather than spread out to the outside of FBIS and FSIS. Thus, the opposite Chern number $\mathcal{C} = +1$ is given by the dynamical field both on FBIS and FSIS.

What we mean here is that no matter how the quenching process is, the TASP only records the topological invariant of the final phase. In fact, the information of initial phase

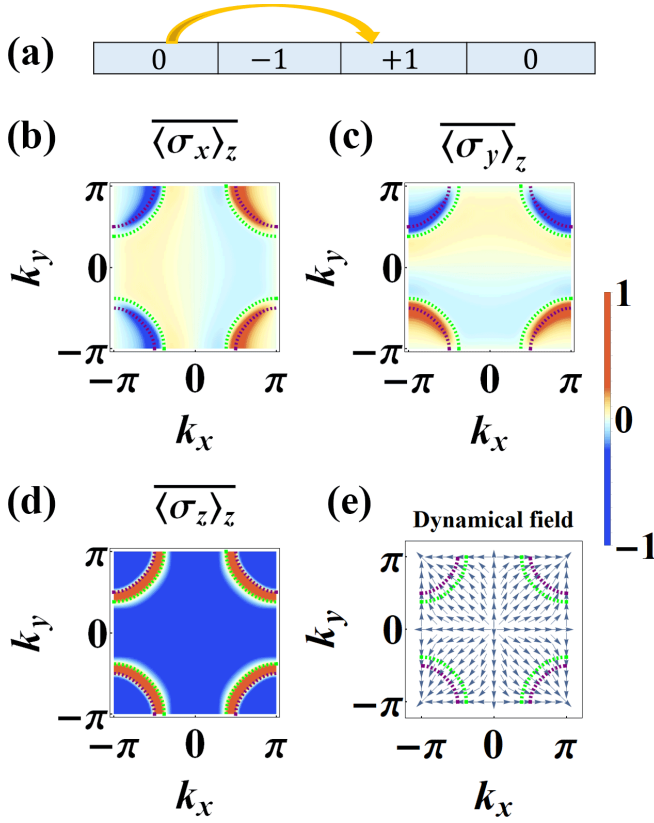


FIG. 2. (a) The specific quenching processes of slow quench. "0" represents the trivial phase, and other numbers represent the topological phases with different topological invariants. (b)-(d) The TASP after quenching h_z axis from a trivial phase to a topological phase with $C = 1$. The system is quenched from $t_i = 1/4$ to $t_f = 5000$ with $5t_{so} = t_0 = g = -m_z = 1$. The quench protocol is g/t and the initial state is the ground state of $\mathcal{H}(t_i)$. (e) The dynamical field of the system plotted by the normalized spin-orbit field.

should also be recorded in the TASP. However, the initial trivial phase here cannot bring any topological information on TASP. Thus, only the information related to final topological phase is recorded in the TASP, and no information during the process is recorded. In experiment, it is no obstacle to obtain bulk topological invariant of the final Hamiltonian based on the winding of the field on the two zero polarizations in $\langle \sigma_z \rangle$, and even no need to distinguish which is the FBIS or FSIS.

B. quench starts from a topological phase to a topological phase

Now, we discuss other processes, which quench from a topological phase to another topological phase. We first start a quench from a topological phase with topological invariant $C = -1$ to a topological phase with topological invariant $C = +1$. As shown in Fig. 3, three vanishing polarizations appear in $\langle \sigma_z \rangle$. The adjacent zero polarizations in $\langle \sigma_z \rangle$ are identified as FBIS and FSIS. Then one can easily distinguish the FBIS and FSIS by the zero polarizations in other components of TASP

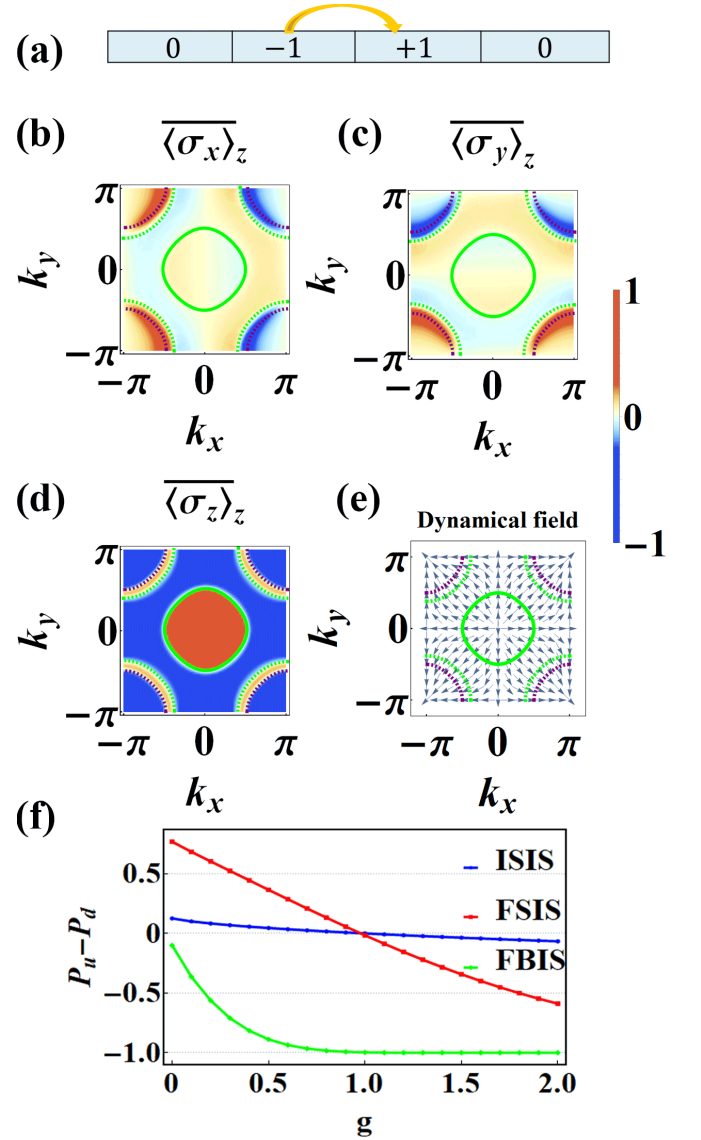


FIG. 3. (a) The specific quenching processes of slow quench. "0" represents the trivial phase, and other numbers represent the topological phases with different topological invariants. (b)-(d) The TASP after quenching h_z axis from a topological phase with $C = -1$ to a topological phase with $C = 1$. The system is quenched from $t_i = 1/2$ to $t_f = 5000$ with $5t_{so} = t_0 = g = m_z = -1$. The quench protocol is g/t and the initial state is the ground state of $\mathcal{H}(t_i)$. The solid green line represents the position of ISIS. (e) The dynamical field of the system plotted by the normalized spin-orbit field. (f) The transition probability of the initial ground state to the final excited state and final ground state in the quenches between different topological regime on ISIS, FSIS, FBIS, respectively.

$\langle \sigma_{x,y} \rangle$. For FBIS, there is no more zero polarizations in other components of TASP, and thus we identify the purple dashed line as FBIS. For FSIS, the zero polarizations can be found in other components of TASP, and thus we identify the green dashed line as FSIS. Naturally, the remaining zero polarization in $\langle \sigma_z \rangle$ is identified as ISIS, which is also denoted by the purple solid line. The numerical results of the transition probability on

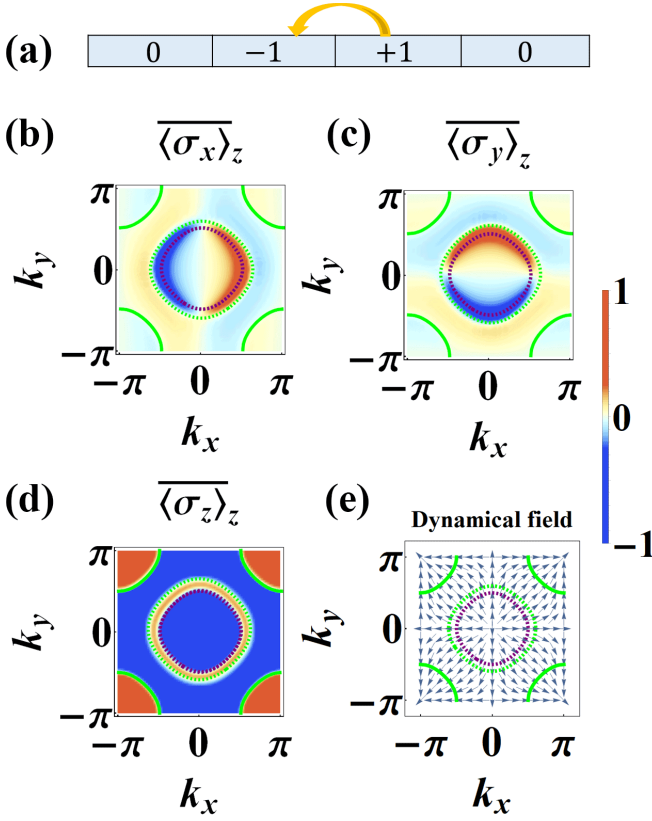


FIG. 4. (a) The specific quenching processes of slow quench. "0" represents the trivial phase, and other numbers represent the topological phases with different topological invariants. (b)-(d) The TASP after quenching h_z axis from a topological phase with $C = 1$ to a topological phase with $C = -1$. The system is quenched from $t_i = 1/2$ to $t_f = 5000$ with $5t_{so} = t_0 = g = m_z = 1$. The quench protocol is $-g/t$ and the initial state is the ground state of $\mathcal{H}(t_i)$. (e) The dynamical field of the system plotted by the normalized spin-orbit field.

three zero polarizations are also shown in Fig. 3(f). The equal transition probability can only be found on the SIS. As the dynamical field plotted in Fig. 3(e), the topology of the final Hamiltonian $\mathcal{H}(t_f)$ can still be characterized from the winding of the dynamical field on the FSIS and FBIS. Meanwhile, the topological invariant related to initial Hamiltonian $\mathcal{H}(t_i)$ is also captured by the winding of the dynamical field on the ISIS.

The above characterization schemes remain valid for the quench starts from a topological phase with topological invariant $C = +1$ to a topological phase with topological invariant $C = -1$. In order to reverse the quenching process, we change the quench protocol g/t as $-g/t$. As shown in Fig. 4, the initial topological phase and the final topological phase with topological invariant $+1$ or -1 can still be characterized by the dynamical field on the FSIS (FBIS) and ISIS, respectively. As long as the initial and final phases of one quenching process are in the same phases as the initial and final phases of another quenching process, respectively, the results of TASP of two quenching processes will be similar.

Note that why we can distinguish the initial phase and final phase is due to the identification of FSIS, FBIS and ISIS. One can imagine how awkward the situation would be if these zero polarizations could not be identified. Compared with the sudden quench (shown in Discussion V), one can really feel the advantages of our characterization schemes.

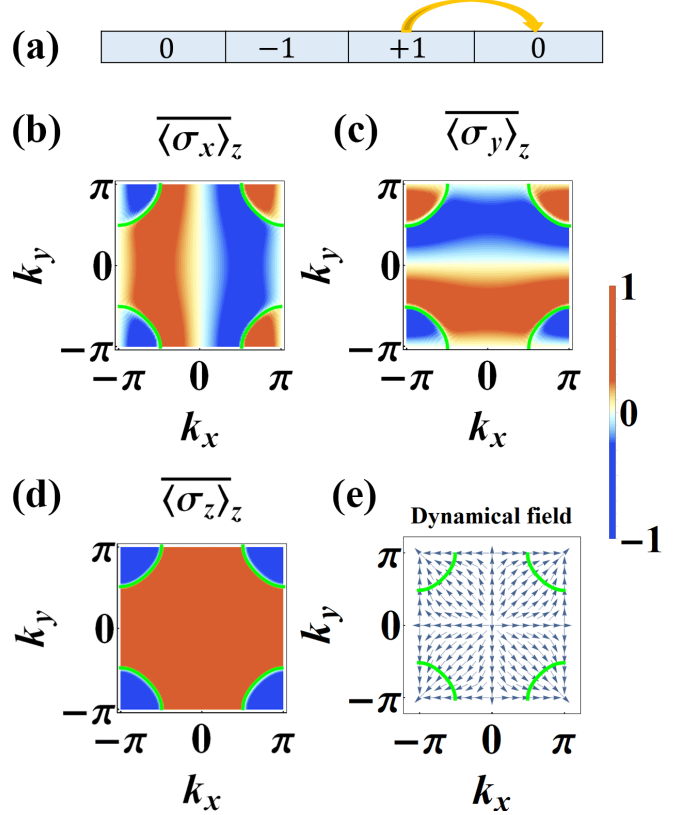


FIG. 5. (a) The specific quenching processes of slow quench. "0" represents the trivial phase, and other numbers represent the topological phases with different topological invariants. (b)-(d) The TASP after quenching h_z axis from a topological phase with $C = 1$ to a trivial phase. The system is quenched from $t_i = 1/3$ to $t_f = 5000$ with $5t_{so} = t_0 = g = 1, m_z = -4$. The quench protocol is g/t and the initial state is the ground state of $\mathcal{H}(t_i)$. (e) The dynamical field of the system plotted by the normalized spin-orbit field.

C. quench starts from a topological phase to a trivial phase

All the final phases in above quenching processes are topological, we further explore how the results are in a reversed quenching process. The results of the quench starts from a topological phase with topological invariant $C = +1$ to a trivial phase are shown in Fig. 5. Here, only one polarization (purple solid line) is observed in the TASP, however, we can still obtain the bulk topological invariant of initial phase $C = +1$ by the winding of the field on this zero polarization. Obviously, this zero polarization is the ISIS due to the fact that the FBIS and FSIS is always appeared at the same time. In other words, there is actually no FBIS exists, and thus no FSIS. Evidently, the

final trivial phase cannot bring any topological information on the TASP. Thus, the TASP only record the information related to initial topological phase.

Overall, each type of quenching process shows its unique features for the zero polarizations (ISIS, FSIS, BIS) in the TASP, and the winding of the field on these zero polarizations exactly reflects the topological invariants of the system. No matter how the quenching process is, the TASP only records the topological invariants of the initial phase and final phase. In particular, the initial phase and final phase can be distinguished by the difference between ISIS, FSIS and BIS.

In addition, the above results for different quenching processes are general. The reason why the TASP can capture the bulk topology of the system is that it actually records all the information about the Hamiltonian before and after quenching. For a two-level system, all the information about the Hamiltonian are $h_z(t_i)$, $h_z(t_f)$, h_x , and h_y . Thus, in general, one can find the zero points of these axes correspond to the positions of the zero polarizations in the TASP. For example, one can always see the zero points of $h_x = \sin x$ and $h_x = \sin y$ correspond to the zero polarizations on the lines $k_x = 0$ and $k_y = 0$ in $\langle \sigma_{x,y} \rangle_z$, respectively. However, only the initial phase or the final phase is topological, the TASP records the information of $h_z(t_i)$ on ISIS and $h_z(t_f)$ on FBIS (FSIS), respectively. We further verify whether the zero points of $h_z(t_i)$ and $h_z(t_f)$ are the same as the positions of the zero polarizations (ISIS, FSIS, FBIS) in the TASP.

As shown in Fig. 6, we extract the TASP on the lines $k_x = k_y$ from the TASP in Fig. 3. The solid lines and dashed lines denote the zero points of $h_z(t_i)$ and $h_z(t_f)$, respectively. One can obviously see the spin polarization $\langle \sigma_z \rangle$ on the solid lines is zero while other polarizations $\langle \sigma_{x,y} \rangle$ is nonzero. Thus, we identify the solid lines as the position of FBIS. That is to say, the position of FBIS is independent on g and always at the zero points of $h_z(t_f)$, i.e., ($h_z = 0$), corresponding to the position of BIS described in previous papers.

The position of FSIS is close to the FBIS, and the spin polarizations on it are all zero. As shown in Fig. 6(b), we denote the change of the position of FBIS by black arrows. Its position depends on the quenching rate g , and totally overlaps with FBIS when $g = 0$. Meanwhile, the nonadiabatic dynamical characterization requires g cannot take a large value. Thus, in a certain range of g ($0 < g < 10$), there would be a FSIS in TASP similar to the shape of FBIS. From the perspective of phase transition, in the process of slow quench, $h_z(\mathbf{k}, t)$ varies with time, and the bulk gap closes while $h_z = \mathbf{h}_{x,y} = 0$, which leads to a topological phase transition with the topological invariant changed by one. In particular, $\mathbf{h}_{x,y} = 0$ is the position of topological charge, i.e., the common singularity enclosed in the FBIS and FSIS. Analogous to the Gaussian theorem [33, 34], the topological charge is actually a monopole, whose quantized flux through the FBIS or FSIS is viewed as the topological invariant. In other words, the topological charge is dual to the FBIS and FSIS. Thus, one can also determine the final topological invariant of the system by its topological charge.

Finally, the position of ISIS is far from the FBIS, and all the spin polarizations on it are also zero. One can obviously

see the position of ISIS is dependent on g , however, compared with FSIS, the influence of the change of g to its position is very insensitive. The position of ISIS is almost at $h_z(t_i) = 0$.

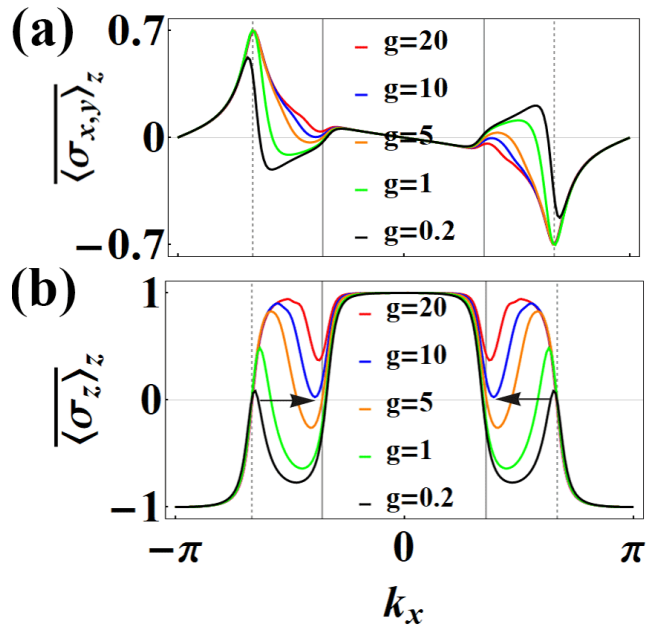


FIG. 6. (a)-(b) The TASP on the line $k_x = k_y$ in the quench between different topological regimes. The positions of ISIS, FBIS are denoted by solid lines, dashed lines, respectively. The change of the position of FSIS is denoted by the arrows.

IV. ROBUSTNESS OF THE RESULTS TO THE INITIAL STATE

All the initial states of the above quenching processes are the ground states of the initial Hamiltonian. It is necessary to explore whether the above results are robust to an arbitrary initial state. As shown below, we plot the TASP in different quenching processes for an arbitrary initial state [superposition state of the ground state and excited state of $\mathcal{H}(t_i)$].

For the quench shown in Fig. 7, we can still identify the purple ring and the green ring as FBIS, FSIS, respectively. The change of initial state only influence the position of FSIS. The FBIS and FSIS still share the same topology, which is ensured by the common topological charge contained in the FBIS and FSIS at $k_x = k_y = 0$. To avoid redundancy, we no longer show the dynamical field below.

For the quenches shown in Fig. 8 and Fig. 9, all the types of the zero polarizations (ISIS, FSIS, FBIS) can be identified according to the features described earlier. Also, we can still know the topological invariants of the initial phase and final phase. The change of initial state only produces another zero polarization similar to ISIS.

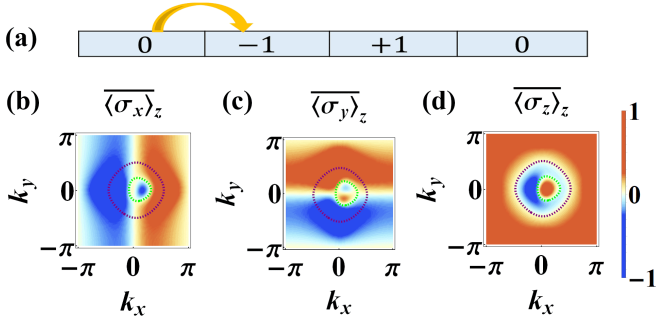


FIG. 7. (a) The specific quenching processes of slow quench. "0" represents the trivial phase, and other numbers represent the topological phases with different topological invariants. (b)-(d) The TASP after quenching h_z axis from a deep trivial phase to a topological regime with $C = +1$. The quench protocol is g/t and the initial state is the superposition state $|\uparrow\rangle + 0.5|\downarrow\rangle$ of $\mathcal{H}(t_i)$. Other parameters keep unchanged. (e) The dynamical field of the system plotted by the normalized spin-orbit field.

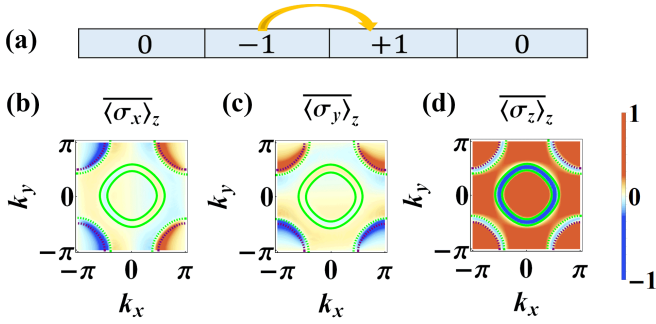


FIG. 8. (a) The specific quenching processes of slow quench. "0" represents the trivial phase, and other numbers represent the topological phases with different topological invariants. (b)-(d) The TASP after quenching h_z axis from a topological phase with $C = -1$ to a topological regime with $C = +1$. The quench protocol is g/t and the initial state is the superposition state $|\uparrow\rangle + |\downarrow\rangle$ of $\mathcal{H}(t_i)$. Other parameters keep unchanged.

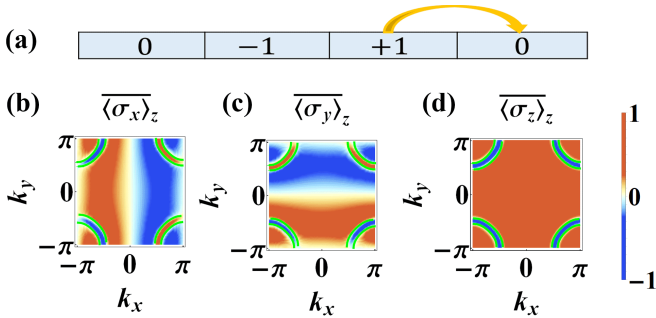


FIG. 9. (a) The specific quenching processes of slow quench. "0" represents the trivial phase, and other numbers represent the topological phases with different topological invariants. (b)-(d) The TASP after quenching h_z axis from a topological regime with $C = -1$ to a trivial phase. The quench protocol is g/t and the initial state is the superposition state $|\uparrow\rangle + |\downarrow\rangle$ of $\mathcal{H}(t_i)$. Other parameters keep unchanged.

V. DISCUSSION

The dynamical characterization schemes we discussed above are only based on the TASP itself, and thus one can easily obtain the topological information of the system from our schemes in experiment. The key point of this paper is: in the framework of slow quench, identifiable zero polarizations (ISIS, FSIS, and FBIS) in TASP give more clear information of the phases we are characterizing. One does not need to know the prior knowledge that the quenches have undergone even how the initial state is before quenching.

To prove this, we also present the results of different quenching processes in sudden quench. One can obviously see from Fig. 10 and Fig. 11, there is no difference for zero polarizations between two reversed quenching processes. In fact, all the zero polarizations in sudden quench have same features in TASP. Therefore, one cannot distinguish the initial phase and final phase even though their topological invariants have already recorded in TASP. As shown in Fig. 12, although the topological invariants of the initial phase and final phase are captured by the winding of the field on purple dashed line and purple solid line, respectively, they cannot be distinguished.

VI. CONCLUSIONS

In summary, take the 2D Chern insulator as a example, we uncover the dynamical characterization in all possible quenching processes. We show that each type of quenching process shows its own features for the zero polarizations in the TASP. One can obtain the topological invariants of initial phase and final phase from the zero polarizations in the TASP. Compared with the sudden quench, the initial phase and final phase can be distinguished by the difference between ISIS, FSIS and FBIS. In a word, no the prior knowledge of the specific quenching process and even the initial state, one can obtain all the topological information from the zero polarizations in the TASP. It is worthwhile that the dynamical characterization schemes here is only based on the TASP itself, and thus one can expect our characterization schemes may provide more reference for future experiments.

ACKNOWLEDGEMENTS

The authors are grateful for the helpful discussions with other members of Research Group of Fuxiang Li. This work was supported by the National Key Research and Development Program of Ministry of Science and Technology (No. 2021YFA1200700), National Natural Science Foundation of China (No. 11905054, and No.11804122), the China Postdoctoral Science Foundation (Grant No. 2021M690970) and the Fundamental Research Funds for the Central Universities from China.

Appendix A: The TASP and dynamical field in nonadiabatic quench dynamics

In *sudden quench*, a two-level Hamiltonian can be written as:

$$\mathcal{H} = \mathbf{h} \cdot \boldsymbol{\sigma} = \begin{pmatrix} \varepsilon \cos \theta & \varepsilon \sin \theta e^{-i\varphi} \\ \varepsilon \sin \theta e^{i\varphi} & -\varepsilon \cos \theta \end{pmatrix}. \quad (\text{A1})$$

Here, ε is the energy of the Hamiltonian. The parameters θ and ϕ are space angles that describe the direction of the effective field \mathbf{h} .

The evolution of state vector can be written as: $|\psi(t)\rangle = e^{-i\mathcal{H}t}|\psi(0)\rangle$. In addition, an arbitrary initial state can be expressed as the superposition state of eigenstates of the postquench Hamiltonian: $|\psi(0)\rangle = C_1|+\rangle + C_2|-\rangle$. After some algebras, we show

$$\overline{\langle \boldsymbol{\sigma} \rangle} = (C_1^2 - C_2^2) \frac{h_i}{\varepsilon}. \quad (\text{A2})$$

If one choose the initial state as the ground state of the initial Hamiltonian $\mathcal{H}_{\theta_0, \varphi_0}$, the TASP will become

$$\overline{\langle \boldsymbol{\sigma} \rangle} = [-\cos(\theta - \theta_0) - \sin \theta \sin \theta_0 (\cos(\varphi - \varphi_0) - 1)] \frac{h_i}{\varepsilon}.$$

Especially, if the initial phase is a deep trivial phase, i.e., far from the phase boundary, the initial ground state will be a completely polarized state along the negative axis of h_0 , and thus the parameter $\theta_0 = 0$. Then the TASP becomes

$$\overline{\langle \boldsymbol{\sigma} \rangle} = -\cos \theta \frac{h_i}{\varepsilon} = -\frac{h_0 h_i}{\varepsilon^2}. \quad (\text{A3})$$

Overall, whatever the initial states we choose, the vanishing spin polarizations in each component of TASP can be two cases: one is the common spin polarizations $C_1^2 - C_2^2 = 0$, the other is unique spin polarizations $h_i = 0$. Here, we define the direction k_{\perp} to be perpendicular to the common spin polarizations ($C_1^2 - C_2^2 = 0$). Thus, the dynamical field on the ($C_1^2 - C_2^2 = 0$) can be shown to be proportional to the spin-orbit field:

$$\partial_{k_{\perp}} \overline{\langle \gamma_{so,i} \rangle} \propto \lim_{k_{\perp} \rightarrow 0} \frac{1}{2k_{\perp}} \frac{h_{so,i} + O(k_{\perp})}{\varepsilon + O(k_{\perp})} 2k_{\perp} = \frac{h_{so,i}}{\varepsilon}. \quad (\text{A4})$$

In *slow quench*, due to the same initial phase can correspond to different time starting points t_i , we cannot give the explicit expression of the TASP in different quenching processes. However, as mentioned in the main text, we can always observe some zero polarizations on the lines $k_x = 0$ and $k_y = 0$ in the

TASP $\overline{\langle \gamma_{1,2} \rangle}$. That is to say, the information of h_1 and h_2 (spin-orbit field $h_{so,i}$) are always recorded in TASP $\overline{\langle \gamma_{so,i} \rangle}$. Thus, similar to the sudden quench, the TASP $\overline{\langle \gamma_{so,i} \rangle}$ in slow quench can be qualitatively given by spin-orbit field multiplies by the expression of some zero polarizations (ISIS, FSIS, FBIS):

$$\overline{\langle \gamma_{so,i} \rangle} \cong ZP \cdot (P_u - P_d) \frac{h_{so,i}}{\varepsilon}. \quad (\text{A5})$$

with ZP is the specific expression of zero polarizations in different quench processes. Then one can also show the dynamical field is proportional to spin-orbit field $h_{so,i}$ as sudden quench.

For example, for the quench starts from a topological phase to a topological phase, the TASP can be approximately given by

$$\overline{\langle \gamma_0 \rangle} \cong h_0(t_i)(P_u - P_d) \frac{h_0(t_f)}{\varepsilon}. \quad (\text{A6})$$

$$\overline{\langle \gamma_{so,i} \rangle} \cong h_0(t_i)(P_u - P_d) \frac{h_{so,i}}{\varepsilon}. \quad (\text{A7})$$

Here, the zero polarizations in $\overline{\langle \gamma_0 \rangle}$ are $h_0(t_i) = 0$, $P_u - P_u = 0$, and $h_0 = 0$, which correspond to the ISIS, FSIS, and FBIS, respectively. When g tends to zero, the position of FBIS overlaps with FBIS, and thus $P_u - P_d$ becomes $\frac{h_0(t_f)}{\varepsilon}$. A direct verification can be made by comparing this formula with the TASP of sudden quench.

Appendix B: The different quench processes in sudden quench

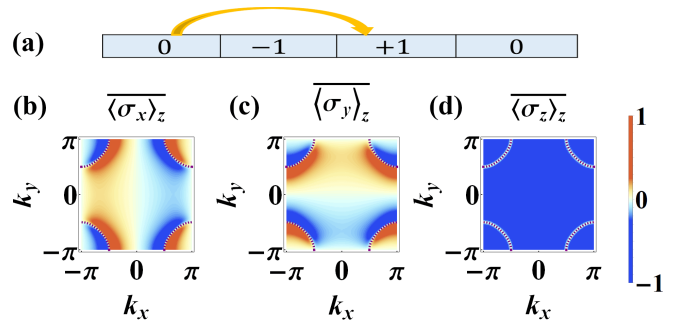


FIG. 10. (a) The specific quenching processes of sudden quench. "0" represents the trivial phase, and other numbers represent the topological phases with different topological invariants. (b)-(d) The TASP after suddenly quenching h_z axis from a trivial phase to a topological phase with $C = -1$. The system is quenched from $m_z = 4$ to $m_z = -1$ with $5t_{so} = t_0 = 1$. The initial state is the ground state of $\mathcal{H}(m_z = 4)$.

[1] M. Z. Hasan and C. L. Kane, *Rev. Mod. Phys.* **82**, 3045 (2010).
 [2] X. L. Qi and S.-C. Zhang, *Rev. Mod. Phys.* **83**, 1057 (2011).

[3] M. C. Rechtsman, J. M. Zeuner, Y. Plotnik, Y. Lumer, D. Podolsky, F. Dreisow, S. Nolte, M. Segev, and A. Szameit, *Nature* **496**, 196 (2013).

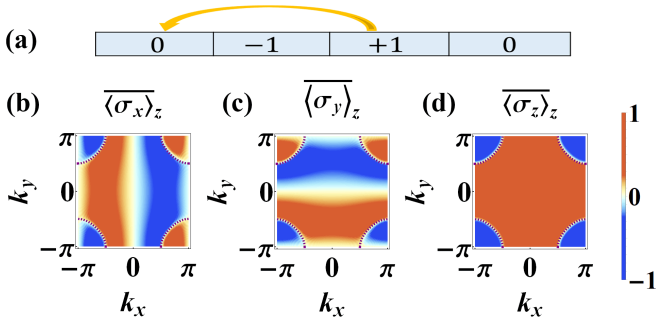


FIG. 11. (a) The specific quenching processes of sudden quench. "0" represents the trivial phase, and other numbers represent the topological phases with different topological invariants. (b)-(d) The TASP after suddenly quenching h_z axis from a topological phase to a trivial phase with $C = -1$. The system is quenched from $m_z = -1$ to $m_z = 4$ with $5t_{so} = t_0 = 1$. The initial state is the ground state of $\mathcal{H}(m_z = -1)$.

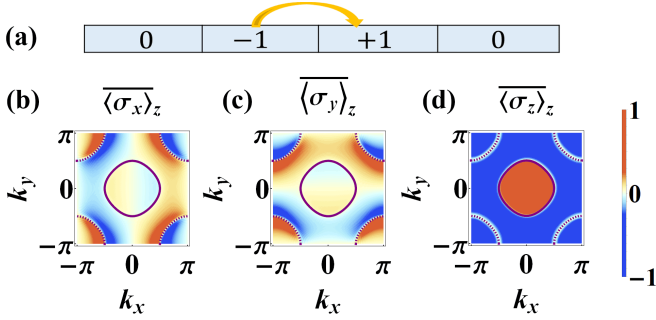


FIG. 12. (a) The specific quenching processes of sudden quench. "0" represents the trivial phase, and other numbers represent the topological phases with different topological invariants. (b)-(d) The TASP after suddenly quenching h_z axis from a topological phase with $C = 1$ to a topological phase with $C = -1$. The system is quenched from $m_z = 1$ to $m_z = -1$ with $5t_{so} = t_0 = 1$. The initial state is the ground state of $\mathcal{H}(m_z = 1)$.

[4] A. B. Khanikaev, S. Hossein Mousavi, W.-K. Tse, M. Kargarian, A. H. MacDonald, and G. Shvets, *Nat. Mater.* **12**, 233 (2013).
 [5] T. Ozawa, H. M. Price, A. Amo, N. Goldman, M. Hafezi, L. Lu, M. C. Rechtsman, D. Schuster, J. Simon, O. Zilberberg, and I. Carusotto, *Rev. Mod. Phys.* **91**, 015006 (2019).
 [6] H. Miyake, G. A. Siviloglou, C. J. Kennedy, W. C. Burton, and W. Ketterle, *Phys. Rev. Lett.* **111**, 185302 (2013).
 [7] G. Jotzu, M. Messer, R. Desbuquois, M. Lebrat, T. Uehlinger, D. Greif, and T. Esslinger, *Nature (London)* **515**, 237 (2014).
 [8] Y.-X. W and F.-X. Li, *Phys. Rev. B.* **104**, 035202 (2021).
 [9] D. Hsieh, D. Qian, L. Wray, Y. Xia, Y. S. Hor, R. J. Cava, and M. Z. Hasan, *Nature* **452**, 970 (2008).

[10] Y. Xia, D. Qian, D. Hsieh, L. Wray, A. Pal, H. Lin, A. Bansil, D. Grauer, Y. S. Hor, R. J. Cava, and M. Z. Hasan, *Nat. Phys.* **5**, 398 (2009).
 [11] C.-Z. Chang, J. Zhang, X. Feng, J. Shen, Z. Zhang, M. Guo, K. Li, Y. Ou, P. Wei, L.-L. Wang, Z.-Q. Ji, Y. Feng, S. Ji, X. Chen, J. Jia, X. Dai, Z. Fang, S.-C. Zhang, K. He, Y. Wang, L. Lu, X.-C. Ma, and Q.-K. Xue, *Science* **340**, 167 (2013).
 [12] S.-Y. Xu, I. Belopolski, N. Alidoust, M. Neupane, G. Bian, C. Zhang, R. Sankar, G. Chang, Z. Yuan, C.-C. Lee, S.-M. Huang, H. Zheng, J. Ma, D. S. Sanchez, B. Wang, A. Bansil, F. Chou, P. P. Shibayev, H. Lin, S. Jia, and M. Z. Hasan, *Science* **349**, 613 (2015).
 [13] B. Zhu, Y. Ke, H. Zhong and C. Lee, *Phys. Rev. Research.* **2**, 023043 (2020).
 [14] L. Zhang, L. Zhang, and X.-J. Liu, *Phys. Rev. Research.* **3**, 013229 (2021).
 [15] L. Zhang, L. Zhang, and X.-J. Liu, *Phys. Rev. Lett.* **125**, 183001 (2020).
 [16] L. Zhang, L. Zhang, Y. Hu, N. Sen, and X.-J. Liu, *Phys. Rev. B.* **103**, 224308 (2021).
 [17] L.-H. Li, W.-W. Zhu, and J.-B. Gong, *Sci. Bull.* **66**, 1502 (2021).
 [18] C. Wang, P. Zhang, X. Chen, J. Yu, and H. Zhai, *Phys. Rev. Lett.* **118**, 185701 (2017).
 [19] X. Qiu, T.-S. Deng, Y. Hu, P. Xue, and W. Yi, *iScience* **20**, 392 (2019).
 [20] D. Xie, T.-S. Deng, T. Xiao, W. Gou, T. Chen, W. Yi, and B. Yan, *Phys. Rev. Lett.* **124**, 050502 (2020).
 [21] H. Hu and E. Zhao, *Phys. Rev. Lett.* **124**, 160402 (2020).
 [22] X. Chen, C. Wang, and J. Yu, *Phys. Rev. A.* **101**, 032104 (2020).
 [23] B. Song, C. He, S. Niu, L. Zhang, Z. Ren, X.-J. Liu, and G.-B. Jo, *Nat. Phys.* **15**, 911 (2019).
 [24] L. Zhang, L. Zhang, S. Niu, and X.-J. Liu, *Sci. Bull.* **63**, 1385 (2018).
 [25] L. Zhang, L. Zhang, and X.-J. Liu, *Phys. Rev. A.* **100**, 063624 (2019).
 [26] W. Sun, C.-R. Yi, B.-Z. Wang, W.-W. Zhang, B. C. Sanders, X.-T. Xu, Z.-Y. Wang, J. Schmiedmayer, Y.-J. Deng, X.-J. Liu, S. Chen, and J.-W. Pan, *Phys. Rev. Lett.* **121**, 250403 (2018).
 [27] Y. Wang, W. Ji, Z. Chai, Y. Guo, M. Wang, X. Ye, P. Yu, L. Zhang, X. Qin, P. Wang, F. Shi, X. Rong, D. Lu, X.-J. Liu, and J. Du, *Phys. Rev. A.* **100**, 052328 (2019).
 [28] C.-R. Yi, L. Zhang, L. Zhang, R.-H. Jiao, X.-C. Cheng, Z.-Y. Wang, X.-T. Xu, W. Sun, X.-J. Liu, S. Chen, and J.-W. Pan, *Phys. Rev. Lett.* **123**, 190603 (2019).
 [29] X.-J. Liu, Z.-X. Liu, and M. Cheng, *Phys. Rev. Lett.* **110**, 076401 (2013).
 [30] X.-J. Liu, K. T. Law, and T. K. Ng, *Phys. Rev. Lett.* **112**, 086401 (2014).
 [31] P. Fang, Y.-X. W and F. Li, *Phys. Rev. A.* **106**, 022219 (2022).
 [32] J. Ye and F. Li, *Phys. Rev. A.* **102**, 042209 (2020).
 [33] L. Zhang, L. Zhang, and X.-J. Liu, *Phys. Rev. A.* **99**, 053606 (2019).
 [34] W. Jia, L. Zhang, L. Zhang, and X.-J. Liu, *Phys. Rev. A.* **103**, 052213 (2021).
 [35] Z. Wu, L. Zhang, W. Sun, X.-T. Xu, B.-Z. Wang, S.-C. Ji, *Science* **354**, 83 (2016).